PLUMAGE BALANCES CAMOUFLAGE AND THERMOREGULATION IN HORNED LARKS (*EREMOPHILA ALPESTRIS*)

The authors wish to be identified to the reviewers.

Nicholas A. Mason[1,2], Eric A. Riddell[1,3], Felisha Romero[1], Carla Cicero[1], Rauri C.K. Bowie[1,4]

[1]Museum of Vertebrate Zoology, University of California, Berkeley, California, USA

[2]Museum of Natural Science and Department of Biological Sciences, Louisiana State University, Baton Rouge, Louisiana, USA

[3]Iowa State University, Department of Ecology, Evolution, and Organismal Biology, Ames, Iowa, USA

[4]Department of Integrative Biology, University of California, Berkeley, California, USA

* Corresponding author: mason@lsu.edu

Keywords: Alaudidae, color, background matching, crypsis, homeostasis, near-infrared, patterning, physiology, water balance

Short Title: Camouflage and thermoregulation in larks

Word count: 8639

Article type: Major article for submission to *American Naturalist*

Submission contents: main text, four figures, two tables, supplementary information

Abstract

Animal coloration serves many biological functions and must therefore balance potentially competing selective pressures. For example, many animals have camouflage, in which coloration matches the visual background against which predators scan for prey. However, different colors reflect different amounts of solar radiation and may therefore have thermoregulatory implications as well. In this study, we examined geographic variation in dorsal patterning, color, and solar reflectance among Horned Larks (*Eremophila alpestris*) of the western United States. We found associations between dorsal plumage brightness, hue, and patterning relative to the soil conditions where specimens were collected. Specifically, brighter dorsal plumage corresponded to brighter soil, while redder, more saturated hues in dorsal plumage corresponded to redder soils. Furthermore, backs with more high-contrast patterning were more common among females and also associated with soil that had coarser soil fragments, suggesting that lark plumage has been selected to optimize background matching in different environments. We also found that larks exhibited higher solar reflectance in hotter and more arid environments, which lowers the water requirements for homeothermy. Taken together, these findings suggest that natural selection has balanced camouflage and thermoregulation in Horned Larks across a wide variety of soil types and abiotic conditions.

Introduction

Animal colors and patterns constitute complex phenotypes that are shaped by a wide array of biotic and abiotic processes (Burtt 1981; Vo et al. 2011; Cuthill et al. 2017). For example, some species have bright colors involved in sexual selection via mate choice (Andersson and Simmons 2006; Shultz and Burns 2017), whereas others have cryptic colors and patterns driven by natural selection to avoid visual detection by predators (Cott 1944; Endler 1978). Furthermore, animal colors have implications for maintaining homeostasis in different environments due to differences in the reflectance of light wavelengths from solar radiation (Walsberg 1983; Wolf and Walsberg 2000). Thus, animal coloration and patterning must balance multiple selective pressures that may conflict or act synergistically to produce multifunctional phenotypes that vary among populations and species (Caro 2017). Among the wide array of biological processes affecting animal colors, camouflage and thermoregulation are thought to have a particularly strong influence on coloration because of their direct impact on survival.

Camouflage includes a suite of physical and behavioral attributes that deter visual detection by predators and is prevalent among various animal lineages, including arthropods (Farkas et al. 2013; Stevens et al. 2014) and vertebrates (Rosenblum et al. 2009; Isaac and Gregory 2013; Boratyński et al. 2017). Also known as background matching, camouflage favors phenotypes that resemble a random sample of brightness, hue, and patterning of the visual background against which predators actively scan for prey (Endler 1978; Merilaita et al. 1999; Michalis et al. 2017). Thermoregulation is also closely tied to coloration (Walsberg 1983) and sometimes favors phenotypes that either

conflict with background matching (Smith et al. 2016) or that simultaneously enable thermoregulation and camouflage (Wacker et al. 2016). Many species conform to 'Gloger's Rule,' a highly prevalent ecogeographic pattern that ascribes lighter colors to more xeric environments and darker colors to more mesic environments (Gloger 1833; Delhey 2019; Marcondes et al. 2020). This widespread trend is thought to be the product of multiple selective pressures, including camouflage and thermoregulation (Burtt 2004; Delhey et al. 2019). Plumage reflects and absorbs light that includes wavelengths within the visual range of birds (UV-VIS: 300–700 nm) as well as near-infrared wavelengths (NIR: 700–2,600 nm), both of which serve important roles in light and heat absorptance (Stuart-Fox et al. 2017). Within the visual spectrum, darker feathers tend to absorb more light and heat than lighter feathers (Porter and Gates 1969), but the physical properties of feathers and the ability of incident light to travel through or become captured by feather microstructures also play important roles (Walsberg 1988; Wolf and Walsberg 2000). Because NIR wavelengths are not perceived by predators, reflectance at those wavelengths is not related to camouflage but may still play an important thermoregulatory role (Medina et al. 2018).

Despite the prevalence of camouflage among animals, the majority of studies to date on background matching have focused on a small number of systems such as peppered moths (Van't Hof et al. 2011; Cook and Saccheri 2013), pocket mice (Nachman et al. 2003; Linnen et al. 2009), White Sands lizards (Rosenblum et al. 2010; Laurent et al. 2016), and a few ground-nesting birds (Troscianko et al. 2016; Stevens et al. 2017). Most of these systems involve discrete phenotypic variants that occupy visually distinct environments. In comparison, continuous variation in background

matching across environmental gradients has received far less attention (Stevens and Merilaita 2009; Caro et al. 2016). Furthermore, studies that simultaneously examine camouflage and thermoregulation remain scarce, especially among endotherms, such as birds. Finally, the role of NIR reflectance in potentially mediating tradeoffs between camouflage and thermoregulation remain largely unexplored (Stuart-Fox et al. 2017; Medina et al. 2018).

To address these knowledge gaps, we examined associations between plumage reflectance and patterning, soil color and composition, and thermoregulatory models among geographically variable populations in a widespread songbird, the Horned Lark (*Eremophila alpestris*). Horned Larks occupy a wide variety of open mesic and arid habitats, including deserts, fallow agricultural land, tundra, and grasslands (Beason 1995; Mason et al. 2020). Horned larks build nests and glean seeds and insects on the ground (Wiens and Rotenberry 1979; de Zwaan and Martin 2018). Due to their preference for habitats with sparse vegetation, larks are thought to rely on substrate matching to avoid avian predators (Donald et al. 2017). Although camouflage in Horned Larks has been discussed anecdotally (Zink and Remsen 1986; Mason and Unitt 2018), associations between phenotypic and environmental variation have not yet been tested rigorously. Larks also exhibit various physiological adaptations to aridity gradients (Tieleman et al. 2003*b*, 2003*a*), making them an excellent system to study interactions between camouflage and thermoregulation. If larks exhibit background matching, we predict that soil conditions will be associated with variation in plumage brightness, color, and patterning. Furthermore, if plumage also plays a thermoregulatory role, we predict

that rates of evaporative water loss and solar reflectance will be associated with variation in aridity and temperature.

To test these predictions, we combined digital photography, color and plumage analyses, full-spectrum (UV, Visual, NIR) spectroradiometry of museum specimens, remote sensing data, and simulation-based thermoregulatory models of heat flux to examine phenotype-environment associations between plumage coloration and patterning, soil conditions, and climate. This approach allows us to disentangle the effects of camouflage, thermoregulation, and sexual dimorphism in driving the evolution and ecology of lark coloration. More broadly, it illustrates how we can understand limits on the adaptive potential of certain traits such as coloration. For example, warming climates might select for more reflective features, but at a cost to background matching. Likewise, habitat alterations might select for darker feathers that impose greater physiological stress under warming climates. Thus, one selective pressure might have detrimental effects to another in the evolution of phenotypes. Only by integrating both background matching and thermoregulatory performance can we understand evolutionary responses to these different and potentially competing selective pressures.

Methods

Digital Photography and Image Analysis

We photographed the dorsal side of 270 Horned Lark specimens from the Museum of Vertebrate Zoology (MVZ) at the University of California, Berkeley (Supplementary Table S1), using a Nikon D7000 camera modified for full-quartz calibration (Advanced Camera Services, Watton, Norfolk, England). We measured up to

10 males and 10 females of 17 different subspecies (Figure 1) in the western United States, preferentially selecting specimens from breeding months (May–August) and with undamaged plumage. We used a Novoflex Noflexar 30mm f/3.5 lens, which does not filter out ultraviolet wavelengths and is therefore suitable for measuring plumage reflectance under an avian visual model. We took two RAW images of each specimen at ISO200: one image used a Baader Venus-U filter, which captures wavelengths between ~320–380 nm, and a second image used a Baader UV/IR cut filter, which captures wavelengths between ~400–680 nm. Each image included a ruler at the height of the specimen's dorsal plane with 5% and 80% reflectance standards (Labsphere, Hutton, NH, USA). We automatically aligned and linearized images using the Image Calibration Analysis Toolbox (Troscianko and Stevens 2015), which provides a set of plugins for ImageJ (Schneider et al. 2012), and manually drew polygons corresponding to the dorsal region of each specimen in ImageJ (Supplementary Figure S1).

After processing each image and delimiting the dorsal region of interest, we converted the channel readings for the UV and visual images to the cone-catch values of a blue tit visual model (Vorobyev and Osorio 1998). We then converted these cone-catch values into tetracolorspace measurements (Vorobyev et al. 1998; *sensu* Stoddard and Prum 2008) of hue, saturation, and chroma using the package pavo v2.2.0 (Maia et al. 2013, 2019) in the R programming environment (R Core Team 2020). We also measured achromatic brightness (i.e., total reflectance or luminosity across all wavelengths) and calculated an index of patterning via a series of Fast Fourier Transform (FFT) bandpass filters at 49 levels (beginning at 2 pixels and increasing exponentially by $\sqrt[8]{2}$ to 128). FFTs are widely applied in digital image analysis

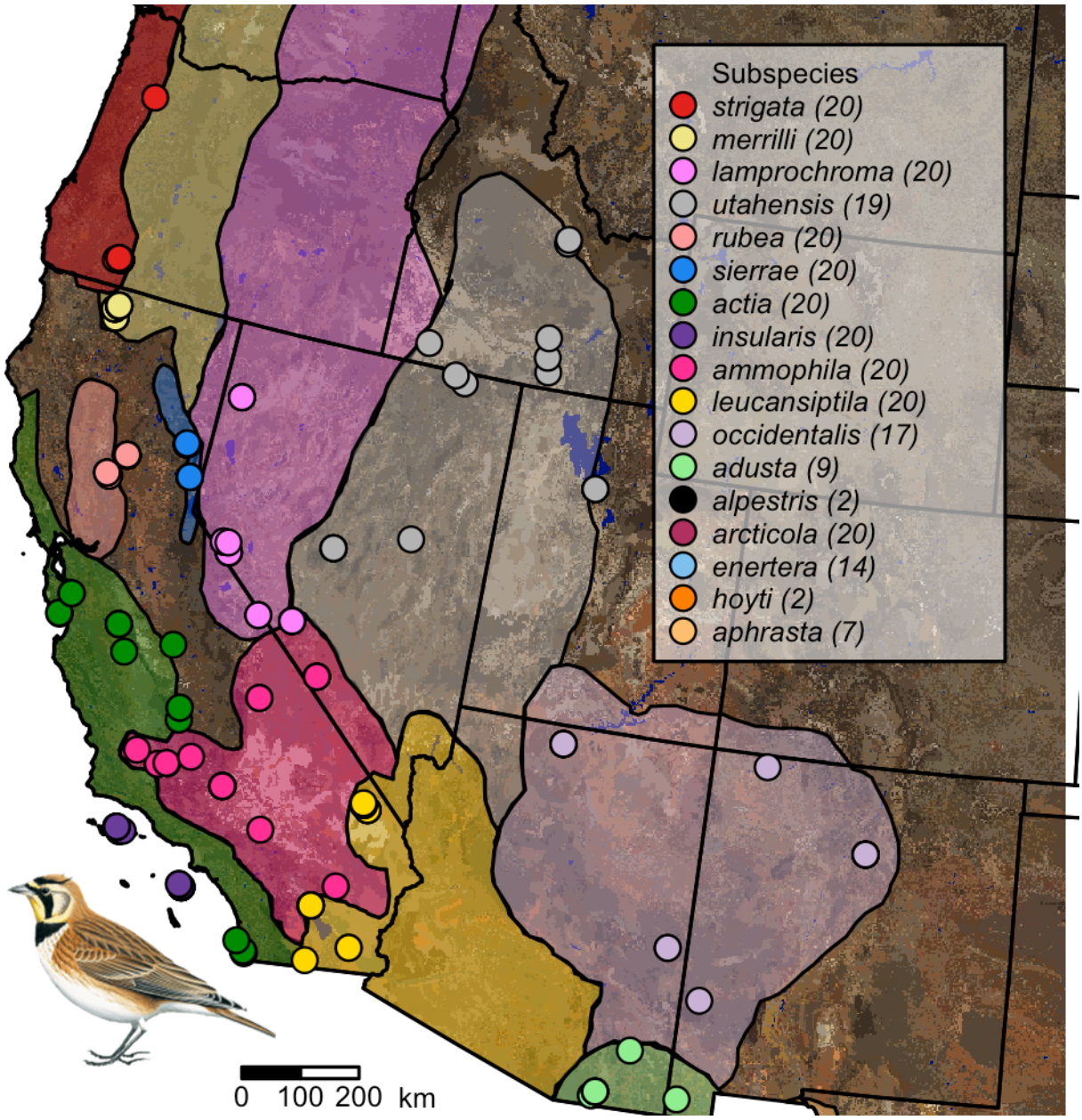

Figure 1: Sampling map showing localities of vouchered Horned Lark (*Eremophila alpestris*) specimens used in this study. Soil color is based on USDA soil surveys, and the approximate range of each subspecies is shown in a different color based on Behle (1942) and new museum records. Some dots may represent more than one individual sampled from the same locality. The number of samples per subspecies is given in parentheses next to the name of the subspecies in the legend in the upper right. Some

subspecies (*alpestris*, *arcticola*, *enertera*, *hoyti*, *aphrasta*) are not shown because we focused on the geographic area with the most dense sampling.

(Stoddard and Osorio 2019) and can be used to quantify animal patterns based on neurophysiological processing of spatial patterns (Godfrey et al. 1987; Stoddard and Stevens 2010; Troscianko et al. 2016; Mason and Bowie 2020). In this process, an image is converted into a set of sine waves, each with a different frequency and amplitude. The amplitude or power of each wave indicates how much patterning—or change between light and dark pixels—occurs at a specific spatial scale. Thus, images with high power across FFT bandwidths display more patterning (e.g. the dorsal spots on some larks), whereas images with lower power are more uniformly colored.

Finally, we performed a principal component analysis on the three focal plumage characters: brightness, achieved chroma, and back patterning (total power) to summarize plumage variation among the sampled larks. We found that the first principal component axis loaded positively with brightness and dorsal patterning, whereas the second principal component axis represented a tradeoff between brightness and back patterning (Supplementary Table S2).

Measuring Full-spectrum Solar Reflectance

We measured solar reflectance of the lark specimens described above using recently published methods for estimating heat stress in birds (Riddell et al. 2019). For each specimen, we measured dorsal and ventral feather reflectance from 350 – 2500 nm using an ASD FieldSpec Pro spectroradiometer (ASD, Inc., 1625 S. Fordam Street,

186 Suite 300, Longmont, CO 80503), and standardized each measurement relative to a
187 Spectralon™ white standard before recording our measurements. We used a custom-
188 built tungsten halogen light source to measure feather reflectance 2 cm from the feather
189 surface, with a 45° angle between the light source and fiber optic cable. This light
190 source was built using an AC-to-DC voltage converter to inhibit interference from an
191 alternating source of electrical current. To standardize the angle and distance, we used
192 a RPH-1 reflection probe holder (Ocean Optics, Inc., Largo, FL). We also used the
193 reflection probe to standardize the surface area of each measurement to ensure that the
194 measurements were not influenced by body size. The combination of numerous
195 measurements per specimen (see below) and the diameter of the probe opening (6.35
196 mm) ensured that we captured the average solar reflectance of each side for each
197 specimen.

198 We used ViewSpec software (ASD, Inc.) to measure solar reflectance, recording
199 ten measurements (five dorsal and five ventral) for each of the 270 specimens. On both
200 the dorsal and the ventral sides, we recorded one measurement from the crown or neck
201 and four measurements spread across the breast or mantle for a total of 2,700
202 measurements. We then used a custom script in Python (v. 3.5) to average these
203 values for each individual, and corrected the reflectance curves for solar radiation using
204 the ASTM G-172 standard irradiance spectrum for dry air provided by SMARTs v. 2.9
205 (Gueymard 2001). We calculated the corrected value by multiplying the intensity of solar
206 radiation by the empirical reflectance, integrating across all of the wavelengths, and
207 dividing by the total intensity of solar radiation (Gates 1980).
208

Remote Sensing Data

We compiled two different soil data sets to examine associations between lark dorsal plumage and soil conditions. First, we downloaded a soil color data set based on an extensive series of United States Department of Agriculture soil surveys of the contiguous United States, with values that had been converted from Munsell color charts to RGB color space (Beaudette et al. 2013). Using georeferenced localities of each lark specimen obtained from the MVZ database Arctos (arctos.database.museum), we extracted their respective soil values and performed a principal components analysis to assess soil color. The first principal component axis loaded strongly with all three channels corresponding to soil brightness. The second principal component axis loaded positively with the red channel, but negatively with blue and green (Supplementary Table S3), and therefore corresponded to soil redness. In this manner, we obtained soil color data associated with the site of collection of 224 of our lark specimens. This soil color dataset is limited to the continental United States, so we were unable to include 46 individuals from populations in Alaska, Canada, and Mexico in this part of our analysis.

We also downloaded harmonized soil property data for the top five centimeters of soil depth at a 30 arc-second resolution from the WISE30Sec database (Batjes 2016). WISE30Sec data has been used widely to study soil biogeochemistry for quantifying global carbon stocks (Sanderman et al. 2017). Although it has not been applied broadly to organismal biology, this dataset provides ecologically relevant information on clay abundance, proportion of coarse fragments, and other soil properties relevant to terrestrial organisms such as Horned Larks. To generate an index of soil surface

granularity, we extracted the volume percentage of coarse fragments (> 2 mm) and the mass percentages of sand, silt, and clay. We then performed a principal component analysis and found that the first principal component axis loaded positively with coarse fragments and sand, and negatively with silt and clay (Supplementary Table S4).

To examine associations between climate and plumage, we also downloaded all 19 WorldClim bioclimatic variables (worldclim.org; Hijmans et al. 2005) at a resolution of 30 arc-seconds to examine associations with dorsal plumage. We conducted a principal component analysis in which the first principal component axis loaded positively with seasonality, the second principal component axis loaded positively with aridity, and the third principal component axis loaded positively with temperature (Supplementary Table S4).

Statistical Analyses of Phenotype-Environment Associations

We performed a series of statistical analyses to examine associations between dorsal plumage and the environment. First, we summarized phenotypic variation among subspecies by plotting the first two PCA axes of plumage variation and noted clustering by subspecies and sex. We then compared mean values by first performing an analysis of variance on the output of linear models, with subspecies as the grouping variable and with males and females separately. We subsequently used a Tukey's multiple comparison post-hoc test (Steel et al. 1997) with the HSD test function from the agricolae package v1.3-3 (de Mendiburu 2020) in R (v4.0.1; R Core Team 2020) to assign subspecies to groups within each sex based on their mean values. We then constructed linear models (LMs) to quantify background matching by examining

associations between plumage and soil variables with sex included as a main effect. Specifically, we constructed the following LMs: (1) plumage brightness as the response variable with soil brightness (soil color PC1) and sex as main effects; (2) plumage redness as the response variable with soil redness (soil color PC2) and sex as main effects; and (3) plumage patterning as the response variable with soil granularity (soil composition PC1) and sex as main effects. We also calculated Pearson's product-moment correlation coefficients between plumage brightness and soil brightness (soil color PC1), plumage chroma and soil redness (soil color PC2), and plumage patterning (plumage patterning PC1) and soil granularity (soil granularity PC1) using the cor.test() function in R (v4.0.1; R Core Team 2020).

Finally, we generated additional LMs to simultaneously estimate the influence of soil and bioclimatic conditions on variation in plumage reflectance. Specifically, we constructed a LM with dorsal brightness (UV-VIS) as a response variable and soil color, seasonality, aridity, temperature, and sex as main effects using the glm() function in R (R Core Team 2020). We also generated a LM with dorsal solar reflectance (UV-VIS-IR) as a response variable and soil color, seasonality, aridity, temperature, and sex as main effects with the same function and settings.

Heat flux simulations

We incorporated the empirical measurements of solar-corrected feather reflectance into a heat flux model to estimate the thermoregulatory differences among subspecies. This model simulates heat balance using the morphological characteristics

277 of the bird in a complex radiative and thermal environment. The simulation output
278 produces estimates of net sensible heat flux (Q), which was calculated using:
279

$$Q = M - E - C\frac{dT_b}{dt} = K_e(T_b - T_e) \quad \text{Eq. 1}$$

280
281

282 where M is the heat generated through metabolic processes, E is the heat lost via
283 evaporative processes, T_b is body temperature, K_e is the effective conductance, and T_e
284 is the operative temperature. The net sensible heat flux equation estimates the heat flux
285 required to maintain a stable body temperature given the morphology of the bird and its
286 interaction with the environment.

287 The heat flux simulation uses biophysical principles to estimate heat flux between
288 the birds and their environment. We used environmental data generated by *NicheMapR*
289 (v1.1.3; Kearney and Porter 2020) to estimate the thermal microclimate for larks. First,
290 we obtained monthly minimum and maximum air temperatures from the *Worldclim*
291 global climate database for the sites at which specimens had been collected. We then
292 corrected these temperatures using *NicheMapR* to reflect conditions relevant to larks,
293 using a reference height of 5 cm above the ground because larks spend most of their
294 time near the ground. We simulated heat flux assuming two types of soil environments:
295 a xeric, desert-like environment (sand, soil reflectance = 0.35) and a more mesic
296 environment (loam, soil reflectance = 0.15; Campbell and Norman 1998). These two
297 environments represent the extremes of the thermal environment that larks inhabit in
298 our study area. Assuming a more reflective soil (i.e., sand) in our simulations did not
299 qualitatively alter our conclusions. We then used these environments to understand the

thermal consequences of variation in dorsal and ventral solar-corrected feather reflectance.

We incorporated morphological phenotypes that directly influence reflected solar radiation in several ways. Our goal was to isolate the importance of dorsal reflectance for thermoregulation. Thus, we assumed that each phenotype was equivalent among subspecies, with the exception of feather reflectance. In general, variation in body mass among subspecies of western Horned Larks is low (males = 29.7 g ± 2.4, females = 28.5 ± 3.5 g; Behle 1942), suggesting that the differences in mass are unlikely to substantially influence thermoregulatory differences among subspecies. Estimates of morphological phenotypes were taken from Riddell et al. (2019) using three specimens that represented the average mass of a lark in our simulations, but here we briefly describe the methods. We estimated plumage depth (sensu Kearney et al. 2016) by measuring the vertical distance from the skin to the outer surface of the feathers using a Fisherbrand™ 150 mm ruler at 10 locations that spanned the dorsal and ventral side of each specimen. We also measured the average length of contour feathers across six feathers per specimen spanning the dorsum and ventrum. To characterize the approximate shape of larks, we used measurements of the height, length, and width of the lark specimens. We measured length from crown to the vent, width from shoulder to shoulder, and height from the back of the dorsal side to the breast at the shoulder (Kearney et al. 2019). We then used these values to estimate the rough dimensions of a lark, assuming a spheroid shape (Porter and Kearney 2009). The dimensions of birds in nature are dependent upon posture and are thus highly variable. By using the same dimensions for each subspecies, our analysis focuses on the thermoregulatory effects

of reflectance and avoids possible noise due to specimen preparation and behavioral differences among subspecies. The mean body mass for Horned Larks (29.5 g) was determined by Riddell et al. (2019), which used the Vertnet data aggregator (vertnet.org). Briefly, body mass was based on collection points in western North America (n = 2,468). The protocol in Riddell *et al*. (2019) removed data greater or less than two standard deviations from the mean body mass to remove juvenile values erroneously labelled as adult and extreme outliers that were likely a mistake. Estimates of mass agree closely with previously published values for subspecies of larks (Behle 1942).

The simulation estimates heat flux by integrating morphological phenotypes with environmental biophysics and behavior. Estimating heat flux in endotherms is complicated by properties of the insulation layer. We addressed these issues by integrating a series of equations involved in a two-dimensional heat transfer model to estimate the flux from the dorsal and ventral components of a bird (Bakken 1981). This model calculates the total amount of heat absorbed or lost from the environment, and converts the amount of energy into the physiological response that would be necessary to maintain a stable body temperature (39ºC in our simulations). These values represent the amount of heat that needs to be generated via metabolic heat production or lost via evaporative cooling to regulate body temperature. We incorporated sources of heat specifically including air temperature, direct solar radiation, diffuse solar radiation, reflected radiation from the ground and sky, and longwave radiation from the sky and ground. We also calculated standard operative temperature (T_{es}) to equate simulated environments in the field to laboratory conditions as shown in Equation 2:

$$T_{es} = T_b - \frac{K_e}{K_{es}}(T_b - T_e) \quad \text{Eq. 2}$$

where T_b is body temperature, K_e is effective conductance, K_{es} is standard effective conductance, and T_e is operative temperature. Standard operative temperature equates the heat flux that an organism experiences in a black-body temperature-controlled metabolic chamber under specific convective conditions to that of a complex thermal environment to predict a physiological response. For our simulations, we assumed K_{es} represented the effective conductance at 0.1 m/s for our standard convective conditions. The specific calculations for these simulations can be found in Riddell *et al*. (2019) and the Python script can be found on GitHub (github.com/ecophysiology).

We used these simulations to isolate the thermoregulatory consequences of geographic variation in dorsal feather reflectance. We were specifically interested in estimating the water requirements for evaporative cooling (termed 'cooling costs') because these costs are highly relevant to the environmental pressures shaping physiological adaptation in larks (Tieleman et al. 2003*a*). We estimated cooling costs across all sites with available climate and elevational data (n = 66). For all sites, we generated estimates of cooling costs using two simulations: one with the average dorsal reflectance across all sites (average = 0.65) and the other incorporating the site-specific dorsal reflectance (range = 0.47 – 0.80). Ventral feather reflectance was held constant (average = 0.69) to specifically focus on the role of dorsal feather reflectance in camouflage and thermoregulation. For each site, we subtracted the cooling costs between the two simulations. The difference (termed reduction in cooling costs)

provides an index for the site-specific reduction in thermoregulatory pressure driven by geographic variation in dorsal feather reflectance.

We then determined whether the reduction in cooling costs from geographic variation in reflectance was associated with climatic variables. We fit exponential models from the *nls*() function in *R* (v4.0.1; R Core Team 2020) to determine the relationship between the reduction in cooling costs and the principal components of climatic variables. For climatic variables, we averaged the principal components that described seasonality (PC1), aridity (PC2), and temperature (PC3; see Table S4 for loadings). We converted the principal components to positive values by adding the lowest value to each principal component, which generated interpretable confidence intervals. Starting values for coefficients were generated using the *nlsLM*() function. We assessed the significance of the models based on the regression coefficients, standard errors of coefficients, and 95% confidence intervals. We then used an AIC model selection framework to determine whether models with the principal components of seasonality, aridity, or temperature were more likely to explain the variation in the reduction in cooling costs attributed to variation in feather reflectance.

Results

Phenotypic variation

Plumage characters varied among subspecies and sexes, but also exhibited substantial overlap. The PCA of plumage characters revealed general clustering by both subspecies and sex (Figure 2A). For example, *E. a. leucansiptila* tended to have higher PC1 and PC2 scores, indicating that they were lighter and more patterned compared to

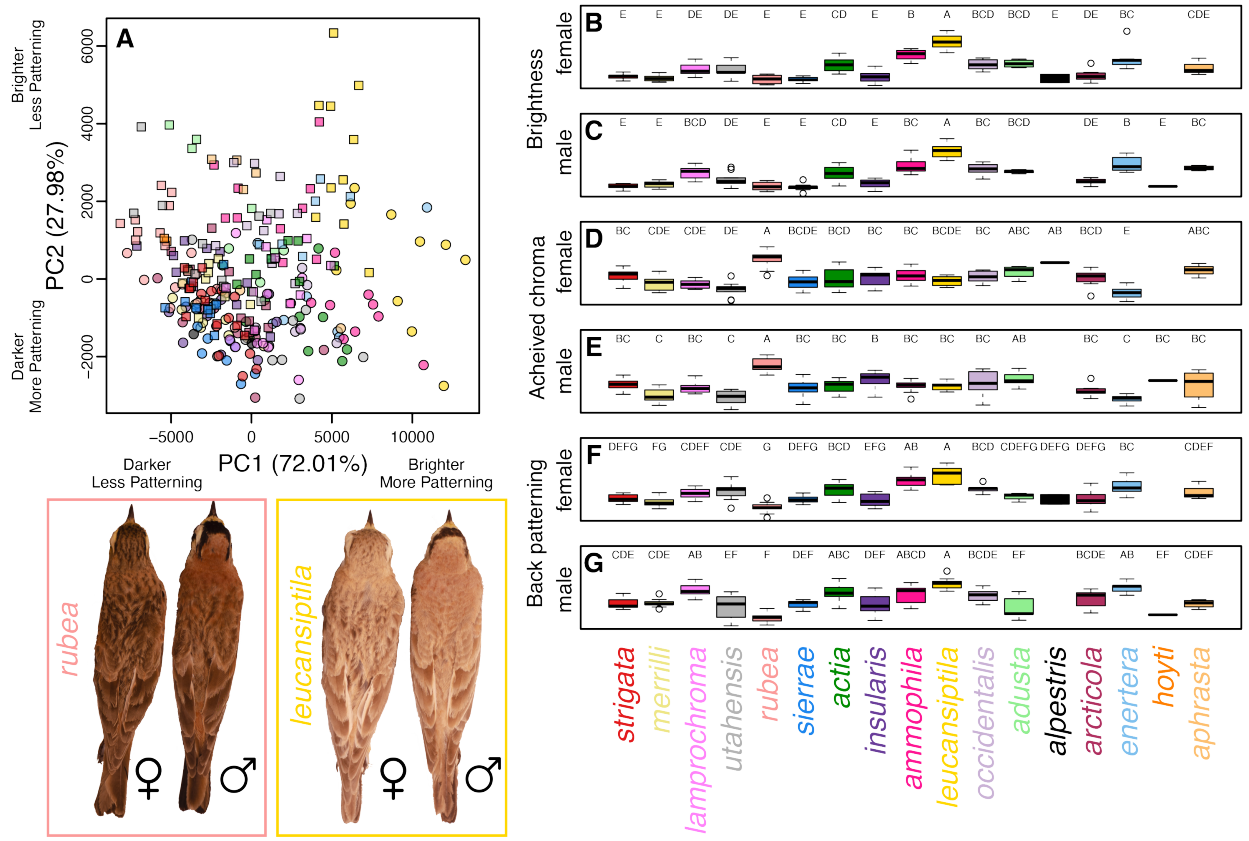

Figure 2: Phenotypic variation in Horned Lark plumage. A principal component analysis (A) reveals clustering by subspecies (colors correspond to labels below boxplots) and sex (males shown with squares, females shown with circles). Panels B–G show box plots of brightness, achieved chroma, and dorsal patterning for males and females. Letters above each boxplot correspond to Tukey's posthoc groupings. Subspecies are ordered to reflect their approximate geographic distributions from northwest to southeast. Inset on the lower left shows is an example of male and female *E. a. rubea* and *E. a. leucansiptila*, which represent opposite ends of the phenotypic distribution of larks included in this study.

other subspecies. Furthermore, males tended to have lower PC1 scores and higher PC2 scores than females, indicating that males tended to have less dorsal patterning

than females on average. Comparisons of mean values using Tukey's posthoc tests revealed various groupings among both male and female larks, but also indicated substantial overlap or gradations in phenotypes among subspecies of Horned Lark (Figure 2B–G). In parallel with PCA scores and loadings, we found that *E. a. leucansiptila* was in its own posthoc grouping for brightness for both males (Figure 2B) and females (Figure 2C). Similarly, *E. a. rubea* tended to differ from other subspecies in mean values for all three plumage variables and was frequently in its own posthoc grouping for both males and females. Box plots also revealed substantial overlap in geographically proximate subspecies. For example, the geographic distribution of *E. a. ammophila* overlaps with *E. a. actia* to the west in south-central California, and the two subspecies exhibited substantial overlap in posthoc groupings. Similar overlap was present in other pairs of geographically proximate subspecies, such as *E. a. occidentalis* and *E. a. adusta*, which come into contact in southern Arizona. These results suggest ample clinal variation among subspecies of Horned Lark, as has been noted elsewhere (Behle 1942).

Phenotype-environment associations

Using linear models, we found multiple associations between dorsal plumage variation and soil conditions underlying background matching in Horned Larks (Figure 3). Specifically, we found that dorsal brightness was positively associated with soil brightness ($\beta_{\text{soil brightness}}$ = 47.17 ± 3.5; t-value = 13.49; P < 0.001) and differed marginally between sexes ($\beta_{\text{sex\_male}}$ = 485.46 ± 250.21; t-value =1.94; P = 0.05). Achieved chroma was positively associated with soil redness ($\beta_{\text{soil redness}}$ = 2e-3 ± 3.32e-4; t-value = 6.02;

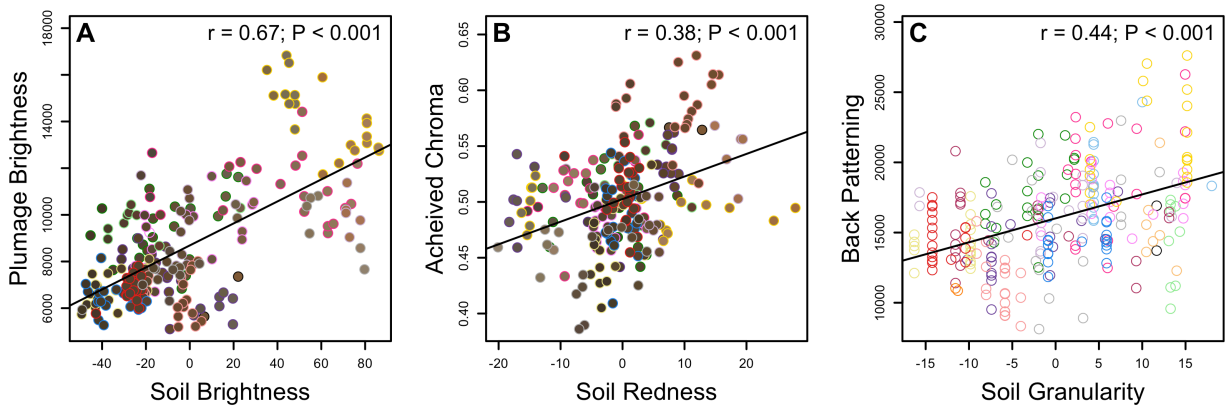

Figure 3: Associations between plumage and soil conditions indicating background matching in Horned Larks. In panels A and B, the fill of each point corresponds to the color of the soil for the locality of the vouchered specimen, which in turn is based on RGB values of USDA soil surveys. The outline of each point corresponds to the subspecies, as seen in Figure 1. Results from Pearson's correlation tests are shown in the upper right hand of each plot. A trend line for the relationship between the two variables is drawn when the Pearson's correlation test is significant ($P < 0.05$).

$P < 0.001$) and differed marginally between sexes (β_{sex_male} = -0.01 ± 5.31e-3; t-value = -1.9; P = 0.06). Finally, we found that dorsal patterning was associated with soil granularity ($\beta_{soil\ granularity}$ = 169.23 ± 19.91; t-value = 8.50; $P < 0.001$) such that dorsal plumages with higher contrast patterning were associated with more granular soils (i.e., more coarse fragments, more clay), and that males were less patterned than females (β_{sex_male} = -2358.47 ± 354.86; t-value = -6.65; $P < 0.001$).

When we expanded our linear models to consider how bioclimatic and soil conditions simultaneously impact dorsal reflectance within the same model, we found a positive association between dorsal plumage brightness (UV-VIS) and soil brightness,

444 seasonality, aridity, and temperature (Table 1). We also found positive associations
445 between dorsal solar reflectance (UV-VIS-IR) and seasonality and aridity, but not
446 between dorsal solar reflectance and soil brightness or temperature (Table 1).
447
448 *Heat Flux Simulations*
449 The observed variation in feather reflectance contributed to a substantial
450 reduction in cooling costs compared to simulations with average feather reflectance.
451 Incorporation of the observed variation in feather reflectance reduced water
452 requirements for evaporative cooling by 15.1% on average (SD = 9.1%; range = 4.1% to
453 70.2%). The reduction in cooling costs was also positively associated with temperature
454 (PC2) and aridity (PC3) indices but not with seasonality (PC1; Figure 4, Table S5).
455 Although the reduction in cooling costs was associated with aridity, model selection
456 indicated that the model with temperature far outperformed models with aridity and
457 seasonality (Table S6).
458
459 **Discussion**
460 By combining data from digital photography, spectroradiometery, and remote
461 sensing we documented multiple associations between dorsal plumage and
462 environmental conditions of Horned Larks over a broad geographic distribution. These
463 findings emphasize the multifarious role of feathers and animal coloration more
464 generally. Although lark coloration has long been hypothesized to facilitate camouflage
465 (Behle 1942; Donald et al. 2017; Mason and Unitt 2018), our study provides the first
466 empirical evidence of phenotype-environment associations that underlie background

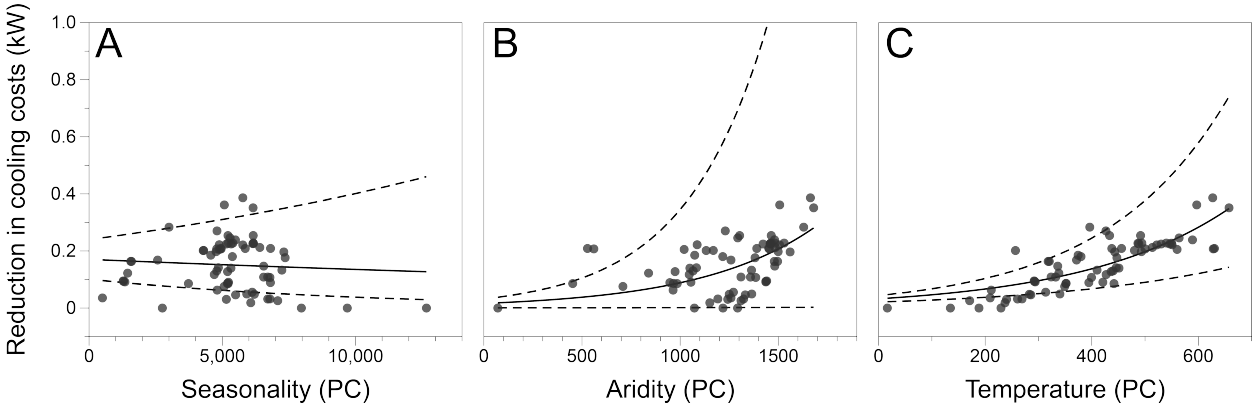

467

468 Figure 4: Variation in feather reflectance reduces thermoregulatory costs in hotter
469 locations. Shown are the relationships between climatic principal components and the
470 reduction in water requirements for evaporative cooling (termed cooling costs) due to
471 variation in dorsal feather reflectance. The reduction in cooling costs was not associated
472 with the principal component for (A) seasonality but was associated with (B) aridity and
473 (C) temperature. The analyses suggest that temperature is a major driver of variation in
474 feather reflectance for thermoregulatory purposes. Exponential models are plotted with
475 95% confidence intervals in the dotted line.

476

477 matching in larks in brightness, hue, and patterning. Furthermore, full-spectrum
478 spectroradiometry combined with simulation-based models of thermoregulation
479 revealed that geographic variation in feather reflectance reduces evaporative cooling
480 costs in hotter environments. While selective pressures imposed on total solar
481 reflectance in feathers have just begun to be explored (Stuart-Fox et al. 2017; Medina et
482 al. 2018), our findings suggest it plays an important role in the thermal ecology of larks.

483 Background matching is one component of a suite of phenotypes that organisms
484 have evolved to avoid visual detection by predators (Merilaita and Lind 2005; Stevens
485 and Merilaita 2009). In order to avoid such detection, natural selection has shaped the

appearance of many organisms so that they resemble a random sample of the background against which their predators typically scan for prey (Endler 1978; Michalis et al. 2017). Dorsal brightness and hue in Horned Larks match the background substrate (Fig. 3A, Fig. 3B), as has also been shown in mice (Vignieri et al. 2010), gerbils (Boratyński et al. 2017), moths (Kettlewell 1955), and other taxa (Stevens et al. 2014; Troscianko et al. 2016). There is less empirical evidence for background matching in pattern as opposed to brightness or color alone, but it has been reported in cuttlefish (Barbosa et al. 2008), nightjars (Troscianko et al. 2016), and plover eggs (Stevens et al. 2017). In Horned Larks, increased dorsal 'mottling' with more high-contrast spots was associated with increases in sand and other coarse particles rather than with clay and silt (Fig. 3C). Beyond background matching, increased dorsal patterning in larks may also contribute to disruptive patterning that breaks up the visual outline of the bird as seen from above (Cuthill et al. 2005). Disruptive patterning in larks may be associated with molt strategies that promote the retention of worn feathers with lighter edges (Negro et al. 2019).

Our study focused on the substrate encountered by Horned Larks during the breeding months. However, migratory populations of larks must avoid detection against multiple, geographically distant substrates that differ in color and composition. Further contributing to the complexity of this challenge, soil color may change over the course of a year as precipitation increases or decreases, especially in more seasonal environments. Horned Larks molt only once per year (Pyle 1997), and thus migratory populations may need to balance competing pressures for background matching against different substrates. Future studies could expand upon our results by examining

how natural selection shapes organisms with non-dynamic camouflage against multiple backgrounds.

We also uncovered associations between climate and dorsal plumage. Specifically, we found that solar reflectance (i.e., UV-VIS-NIR reflectance) is associated with two climatic variables—seasonality and aridity (Table 1)—but bears no association with soil brightness or temperature (Table 1). Thus, solar reflectance increases as climates become more arid, presumably to prevent the organism from overheating and becoming dehydrated. Interestingly, we found greater reductions in cooling costs associated with temperature than with seasonality or aridity (Fig. 4)—an observation that conflicts with implications from our linear models as we found no association between temperature and dorsal solar reflectance in our linear models (Table 1). However, the modeling approach for cooling costs incorporates additional parameters such as NIR reflectance, feather conductance, direct and diffuse solar radiation, and radiation from the ground (Gates 1980). Thus, these findings may not be in direct conflict with one another, but rather may reflect different methodologies and statistical assumptions. Regardless, NIR reflectance might play a role in allowing larks to increase solar reflectance while maintaining crypsis in the visual spectrum. Future work could further disentangle how the NIR and UV-VIS portions of light co-vary or are independently selected for optimal thermoregulation in different climates (Stuart-Fox et al. 2017).

There are many other factors beyond modifications to solar reflectance in UV-VIS and NIR wavelengths that could contribute to the ability of larks to inhabit hot, arid environments (Trost 1972; Dean and Williams 2004). First, many arid-adapted larks

532 have reduced metabolic rates and increased water retention through various
533 physiological adaptations (Tieleman et al. 2002). Second, behavioral adaptations also
534 can reduce heat stress. For example, microhabitat selection such as resting in shade or
535 animal burrows during extreme heat may contribute to thermoregulation in larks
536 (Williams et al. 1999; Hartman and Oring 2003; Walde et al. 2009). While Horned Larks
537 are philopatric and stay close to their breeding territory during the breeding season
538 (Beason 1970), they are nomadic during non-breeding months and may seek out
539 favorable habitat within reach of their individual movements to facilitate
540 thermoregulation. Feathers are one part of a complex suite of phenotypes involved in
541 maintaining homeostasis in thermally challenging environments. The interplay of
542 plumage and other physiological and behavioral adaptations for thermoregulation
543 remains an open avenue of research.

544 In conclusion, our study uncovered empirical evidence for the multifaceted role
545 that plumage plays in mediating both camouflage and thermoregulation in Horned
546 Larks. Dorsal plumage and patterning are associated with soil conditions, whereas
547 feather solar reflectance is associated with abiotic conditions and improved cooling
548 costs in hotter climates. Future studies could leverage these phenotype-environment
549 associations in combination with new genomic resources (Mason et al. 2020) to identify
550 candidate loci driving these local adaptations. Furthermore, Horned Larks are one of
551 approximately 100 species of larks (Alaudidae) globally that vary in habitat affiliations.
552 Phylogenetic comparative studies across the family would shed light on whether the
553 patterns we found here are generalizable across broader taxonomic and evolutionary
554 scales. Interactions between an organisms' body surfaces and light from the sun are

555 complex, and our study illustrates how natural selection has shaped the phenotypic
556 variation across different habitats to meet potentially competing demands.
557
558 **Data and Code Availability**
559 Raw data and code used in the analyses presented here are available via GitHub
560 (https://github.com/mason-lab/HornedLarkCamoThermo). Raw data and metadata will
561 be made available via Dryad upon article acceptance.

562 **References**

563 Andersson, M., and L. W. Simmons. 2006. Sexual selection and mate choice. Trends in
564 Ecology & Evolution 21:296–302.

565 Bakken, G. S. 1981. A two-dimensional operative-temperature model for thermal energy
566 management by animals. Journal of Thermal Biology 6:23–30.

567 Barbosa, A., L. M. Mäthger, K. C. Buresch, J. Kelly, C. Chubb, C.-C. Chiao, and R. T.
568 Hanlon. 2008. Cuttlefish camouflage: The effects of substrate contrast and size in
569 evoking uniform, mottle or disruptive body patterns. Vision Research 48:1242–1253.

570 Batjes, N. H. 2016. Harmonized soil property values for broad-scale modelling
571 (WISE30sec) with estimates of global soil carbon stocks. Geoderma 269:61–68.

572 Beason, R. 1970. *The annual cycle of the Prairie Horned Lark in west-central Illinois*
573 (Master's Thesis). Western Illinois University, Macomb.

574 Beason, R. C. 1995. Horned Lark (Eremophila alpestris), version 2.0. In The Birds of
575 North America (A. F. Poole and F. B. Gill, Editors). Cornell Lab of Ornithology, Ithaca,
576 NY, USA.

577 Beaudette, D. E., P. Roudier, and A. T. O'Geen. 2013. Algorithms for quantitative
578 pedology: A toolkit for soil scientists. Computers & Geosciences 52:258–268.

579 Behle, W. 1942. Distribution and variation of the horned larks (*Eremophila alpestris*) of
580 western North America. University of California Publications in Zoology 46:203–316.

581 Boratyński, Z., J. C. Brito, J. C. Campos, J. L. Cunha, L. Granjon, T. Mappes, A.
582 Ndiaye, et al. 2017. Repeated evolution of camouflage in speciose desert rodents.
583 Scientific Reports 7:1–10.

584 Burtt, E. H. 1981. The adaptiveness of animal colors. BioScience 31:723–729.

585 ———. 2004. GLOGER'S RULE, FEATHER-DEGRADING BACTERIA, AND COLOR
586 VARIATION AMONG SONG SPARROWS. Condor 106:681–686.
587 Campbell, G., and J. Norman. 1998. An introduction to environmental biophysics (2nd
588 edition.). Springer-Verlag, New York, NY.
589 Caro, T. 2017. Wallace on Coloration: Contemporary Perspective and Unresolved
590 Insights. Trends in Ecology & Evolution 32:23–30.
591 Caro, T., T. N. Sherratt, and M. Stevens. 2016. The ecology of multiple colour defences.
592 Evolutionary Ecology 30:797–809.
593 Cook, L. M., and I. J. Saccheri. 2013. The peppered moth and industrial melanism:
594 Evolution of a natural selection case study. Heredity 110:207–212.
595 Cott, H. B. 1944. Adaptive Coloration in Animals. Bradford and Dickens Drayton House,
596 London.
597 Cuthill, I. C., W. L. Allen, K. Arbuckle, B. Caspers, G. Chaplin, M. E. Hauber, G. E. Hill,
598 et al. 2017. The biology of color. Science 357:eaan0221.
599 Cuthill, I. C., M. Stevens, J. Sheppard, T. Maddocks, C. A. Párraga, and T. S.
600 Troscianko. 2005. Disruptive coloration and background pattern matching. Nature
601 434:72–74.
602 de Mendiburu, F. 2020. agricolae: Statistical Procedures for Agricultural Research.
603 de Zwaan, D. R., and K. Martin. 2018. Substrate and structure of ground nests have
604 fitness consequences for an alpine songbird. Ibis 160:790–804.
605 Dean, W. R. J., and J. B. Williams. 2004. Adaptations of birds for life in deserts with
606 particular reference to Larks (Alaudidae). Transactions of the Royal Society of South
607 Africa 59:79–91.

608 Delhey, K. 2019. A review of Gloger's rule, an ecogeographical rule of colour:
609 definitions, interpretations and evidence. Biological Reviews brv.12503.
610 Delhey, K., J. Dale, M. Valcu, and B. Kempenaers. 2019. Reconciling ecogeographical
611 rules: rainfall and temperature predict global colour variation in the largest bird radiation.
612 (G. Grether, ed.)Ecology Letters 22:726–736.
613 Donald, P. F., P. Alström, and D. Engelbrecht. 2017. Possible mechanisms of substrate
614 colour-matching in larks (Alaudidae) and their taxonomic implications. Ibis 159:699–702.
615 Endler, J. A. 1978. A Predator's View of Animal Color Patterns. Evolutionary Biology
616 319–364.
617 Farkas, T. E., T. Mononen, A. A. Comeault, I. Hanski, and P. Nosil. 2013. Evolution of
618 camouflage drives rapid ecological change in an insect community. Current Biology
619 23:1835–1843.
620 Gates, D. 1980. Solar Radiation. Biophysical Ecology, Springer Advanced Texts in Life
621 Sciences. Springer, New York, NY.
622 Gloger, C. W. L. 1833. Das Abändern der Vögel durch Einfluss des Klimas. August
623 Schulz, Breslau, Germany.
624 Godfrey, D., J. N. Lythgoe, and D. A. Rumball. 1987. Zebra stripes and tiger stripes: the
625 spatial frequency distribution of the pattern compared to that of the background is
626 significant in display and crypsis. Biological Journal of the Linnean Society 32:427–433.
627 Gueymard, C. A. 2001. Parameterized transmittance model for direct beam and
628 circumsolar spectral irradiance. Solar Energy 71:325–346.
629 Hartman, C. A., and L. W. Oring. 2003. Orientation and microclimate of horned lark
630 nests: the importance of shade. The Condor 105:158–163.

631 Hijmans, R. J., S. E. Cameron, J. L. Parra, P. G. Jones, and A. Jarvis. 2005. Very high
632 resolution interpolated climate surfaces for global land areas. International Journal of
633 Climatology 25:1965–1978.
634 Isaac, L. A., and P. T. Gregory. 2013. Can snakes hide in plain view? Chromatic and
635 achromatic crypsis of two colour forms of the Western Terrestrial Garter Snake
636 (Thamnophis elegans). Biological Journal of the Linnean Society 108:756–772.
637 Kearney, M. R., and W. P. Porter. 2020. NicheMapR – an R package for biophysical
638 modelling: the ectotherm and Dynamic Energy Budget models. Ecography 43:85–96.
639 Kearney, M. R., W. P. Porter, and S. A. Murphy. 2016. An estimate of the water budget
640 for the endangered night parrot of Australia under recent and future climates. Climate
641 Change Responses 3:14.
642 Kettlewell, H. B. D. 1955. Selection experiments on industrial melanism in the
643 Lepidoptera. Heredity 9:323–342.
644 Laurent, S., S. P. Pfeifer, M. L. Settles, S. S. Hunter, K. M. Hardwick, L. Ormond, V. C.
645 Sousa, et al. 2016. The population genomics of rapid adaptation: disentangling
646 signatures of selection and demography in white sands lizards. Molecular Ecology
647 25:306–323.
648 Linnen, C. R., E. P. Kingsley, J. D. Jensen, and H. E. Hoekstra. 2009. On the origin and
649 spread of an adaptive allele in deer mice. Science 325:1095–1098.
650 Maia, R., C. M. Eliason, P.-P. Bitton, S. M. Doucet, and M. D. Shawkey. 2013. pavo : an
651 R package for the analysis, visualization and organization of spectral data. (A. Tatem,
652 ed.)Methods in Ecology and Evolution n/a-n/a.

653 Maia, R., H. Gruson, J. A. Endler, and T. E. White. 2019. PAVO 2: New tools for the
654 spectral and spatial analysis of colour in R. (R. B. O'Hara, ed.)Methods in Ecology and
655 Evolution 10:1097–1107.
656 Marcondes, R. S., K. F. Stryjewski, and R. T. Brumfield. 2020. Testing the simple and
657 complex versions of Gloger's rule in the Variable Antshrike (Thamnophilus
658 caerulescens, Thamnophilidae). The Auk 137:ukaa026.
659 Mason, N. A., and R. C. K. Bowie. 2020. Plumage patterns: Ecological functions,
660 evolutionary origins, and advances in quantification. The Auk ukaa060.
661 Mason, N. A., P. Pulgarin, C. D. Cadena, and I. J. Lovette. 2020*a*. *De novo* assembly of
662 a high-quality reference genome for the Horned Lark (*Eremophila alpestris*).
663 G3:Genes|Genomes|Genetics 10:475–478.
664 Mason, N. A., and P. Unitt. 2018. Rapid phenotypic change in a native bird population
665 following conversion of the Colorado Desert to agriculture. Journal of Avian Biology
666 49:1–6.
667 Mason, N., P. Unitt, and J. Sparks. 2020*b*. Agriculture induces isotopic shifts and niche
668 contraction in Horned Larks (Eremophila alpestris) of the southern Colorado Desert.
669 Journal of Ornithology In Press.
670 Medina, I., E. Newton, M. R. Kearney, R. A. Mulder, W. P. Porter, and D. Stuart-Fox.
671 2018. Reflection of near-infrared light confers thermal protection in birds. Nature
672 Communications 9:3610.
673 Merilaita, S., and J. Lind. 2005. Background-matching and disruptive coloration, and the
674 evolution of cryptic coloration. Proceedings of the Royal Society B: Biological Sciences
675 272:665–670.

676 Merilaita, S., J. Tuomi, and V. Jormalainen. 1999. Optimization of cryptic coloration in
677 heterogeneous habitats. Biological Journal of the Linnean Society 67:151–161.
678 Michalis, C., N. E. Scott-Samuel, D. P. Gibson, and I. C. Cuthill. 2017. Optimal
679 background matching camouflage. Proceedings of the Royal Society B: Biological
680 Sciences 284.
681 Nachman, M. W., H. E. Hoekstra, and S. D'Agostino. 2003. The genetic basis of
682 adaptive melanism in pocket mice. Proceedings of the National Academy of Sciences of
683 the United States of America 100:5268–5273.
684 Negro, J. J., I. Galván, and J. Potti. 2019. Adaptive plumage wear for increased crypsis
685 in the plumage of Palearctic larks (Alaudidae). Ecology 100.
686 Porter, W. P., and D. M. Gates. 1969. Thermodynamic Equilibria of Animals with
687 Environment. Ecological Monographs 39:227–244.
688 Pyle, P. 1997. Identification Guide to North American Birds. Part I: Columbidae to
689 Ploceidae. Braun-Brumfield, Ann Arbor, Michigan.
690 R Core Team. 2020. R: A language and environment for statistical computing. R
691 Foundation for Statistical Computing, Vienna, Austria.
692 Riddell, E. A., K. J. Iknayan, B. O. Wolf, B. Sinervo, and S. R. Beissinger. 2019. Cooling
693 requirements fueled the collapse of a desert bird community from climate change.
694 Proceedings of the National Academy of Sciences 201908791.
695 Rosenblum, E. B., H. Rompler, T. Schoneberg, and H. E. Hoekstra. 2009. Molecular
696 and functional basis of phenotypic convergence in white lizards at White Sands.
697 Proceedings of the National Academy of Sciences 107:2113–2117.

———. 2010. Molecular and functional basis of phenotypic convergence in white lizards at White Sands. Proceedings of the National Academy of Sciences 107:2113–2117.

Sanderman, J., T. Hengl, and G. J. Fiske. 2017. Soil carbon debt of 12,000 years of human land use. Proceedings of the National Academy of Sciences 114:9575–9580.

Schneider, C. A., W. S. Rasband, and K. W. Eliceiri. 2012. NIH Image to ImageJ: 25 years of image analysis. Nature Methods 9:671–675.

Shultz, A. J., and K. J. Burns. 2017. The role of sexual and natural selection in shaping patterns of sexual dichromatism in the largest family of songbirds (Aves: Thraupidae). Evolution 71:1061–1074.

Smith, K. R., V. Cadena, J. A. Endler, M. R. Kearney, W. P. Porter, and D. Stuart-Fox. 2016. Color Change for Thermoregulation versus Camouflage in Free-Ranging Lizards. The American Naturalist 188:668–678.

Steel, R., J. Torrie, and D. Dickey. 1997. Principles and Procedures of Statistics: A Biometrical Approach. McGraw-Hill.

Stevens, M., A. E. Lown, and L. E. Wood. 2014. Color change and camouflage in juvenile shore crabs Carcinus maenas. Frontiers in Ecology and Evolution 2:1–14.

Stevens, M., and S. Merilaita. 2009. Animal camouflage: current issues and new perspectives. Philosophical Transactions of the Royal Society B: Biological Sciences 364:423–427.

Stevens, M., J. Troscianko, J. K. Wilson-Aggarwal, and C. N. Spottiswoode. 2017. Improvement of individual camouflage through background choice in ground-nesting birds. Nature Ecology & Evolution 1:1325–1333.

Stoddard, M. C., and D. Osorio. 2019. Animal coloration patterns: linking spatial vision to quantitative analysis. The American Naturalist 193:164–186.

Stoddard, M. C., and R. O. Prum. 2008. Evolution of avian plumage color in a tetrahedral color space: a phylogenetic analysis of New World buntings. The American Naturalist 171:755–776.

Stoddard, M. C., and M. Stevens. 2010. Pattern mimicry of host eggs by the Common Cuckoo, as seen through a bird's eye. Proceedings of the Royal Society B: Biological Sciences 277:1387–1393.

Stuart-Fox, D., E. Newton, and S. Clusella-Trullas. 2017. Thermal consequences of colour and near-infrared reflectance. Philosophical Transactions of the Royal Society B: Biological Sciences 372:20160345.

Tieleman, B. I., J. B. Williams, and P. Bloomer. 2003*a*. Adaptation of metabolism and evaporative water loss along an aridity gradient. Proceedings of the Royal Society of London. Series B: Biological Sciences 270:207–214.

Tieleman, B. I., J. B. Williams, and M. E. Buschur. 2002. Physiological Adjustments to Arid and Mesic Environments in Larks (*Alaudidae*). Physiological and Biochemical Zoology 75:305–313.

Tieleman, B. I., J. B. Williams, M. E. Buschur, and C. R. Brown. 2003*b*. PHENOTYPIC VARIATION OF LARKS ALONG AN ARIDITY GRADIENT: ARE DESERT BIRDS MORE FLEXIBLE? Ecology 84:1800–1815.

Troscianko, J., and M. Stevens. 2015. Image calibration and analysis toolbox - a free software suite for objectively measuring reflectance, colour and pattern. (S. Rands, ed.)Methods in Ecology and Evolution 6:1320–1331.

743 Troscianko, J., J. Wilson-Aggarwal, M. Stevens, and C. N. Spottiswoode. 2016.
744 Camouflage predicts survival in ground-nesting birds. Scientific Reports 6:19966.
745 Trost, C. H. 1972. Adaptations of Horned Larks (Eremophila alpestris) to Hot
746 Environments. The Auk 89:506–527.
747 Van't Hof, A. E., N. Edmonds, M. Dalíková, F. Marec, and I. J. Saccheri. 2011. Industrial
748 melanism in british peppered moths has a singular and recent mutational origin.
749 Science 332:958–960.
750 Vignieri, S. N., J. G. Larson, and H. E. Hoekstra. 2010. The selective advantage of
751 crypsis in mice. Evolution 64:2153–2158.
752 Vo, A.-T. E., M. S. Bank, J. P. Shine, and S. V. Edwards. 2011. Temporal increase in
753 organic mercury in an endangered pelagic seabird assessed by century-old museum
754 specimens. Proceedings of the National Academy of Sciences 108:7466–7471.
755 Vorobyev, M., and D. Osorio. 1998. Receptor noise as a determinant of colour
756 thresholds. Proceedings of the Royal Society of London. Series B: Biological Sciences
757 265:351–358.
758 Vorobyev, M., D. Osorio, A. T. D. Bennett, N. J. Marshall, and I. C. Cuthill. 1998.
759 Tetrachromacy, oil droplets and bird plumage colours. Journal of Comparative
760 Physiology A: Sensory, Neural, and Behavioral Physiology 183:621–633.
761 Wacker, C. B., B. M. McAllan, G. Körtner, and F. Geiser. 2016. The functional
762 requirements of mammalian hair: a compromise between crypsis and thermoregulation?
763 The Science of Nature 103:53.

764 Walde, A. D., A. M. Walde, D. K. Delaney, and L. L. Pater. 2009. Burrows of Desert
765 Tortoises (Gopherus agassizii) as Thermal Refugia for Horned Larks (Eremophila
766 alpestris) in the Mojave Desert. The Southwestern Naturalist 54:375–381.
767 Walsberg, G. E. 1983. Coat Color and Solar Heat Gain in Animals. BioScience 33:88–
768 91.
769 ———. 1988. Heat flow through avian plumages: The relative importance of conduction,
770 convection, and radiation. Journal of Thermal Biology 13:89–92.
771 Williams, J. B., B. I. Tieleman, and M. Shobrak. 1999. Lizard Burrows Provide Thermal
772 Refugia for Larks in the Arabian Desert. The Condor 101:714–717.
773 Wolf, B. O., and G. E. Walsberg. 2000. The Role of the Plumage in Heat Transfer
774 Processes of Birds. American Zoologist 40:575–584.
775 Zink, R. M., and J. V. Remsen. 1986. Evolutionary Processes and Patterns of
776 Geographic Variation in Birds. Current Ornithology 4:1–69.
777

778 **Tables**

779 Table 1: Linear model output for plumage-environment associations. *P*-values with

780 asterisks indicate statistically significant terms (*$P < 0.05$; **$P < 0.01$; ***$P < 0.001$).

781

Response Variable	Predictor Variable	Beta + SE	t-value	*P*-value
Dorsal Brightness	Intercept	8420.53 ± 138.09	60.98	<0.001***
	Sex (male)	418.17 ± 192.97	2.17	0.03*
	Soil brightness	18.59 ± 3.58	5.19	<0.001***
	BioClim PC1 (seasonality)	0.17 ± 0.06	2.56	0.01*
	BioClim PC2 (aridity)	4.53 ± 0.38	11.85	<0.001***
	BioClim PC3 (temperature)	5.17 ± 0.92	5.61	<0.001***
Dorsal Solar Reflectance	Intercept	0.34 ± 6.82e-3	49.78	<0.001***
	Sex (male)	1.15e-3 ± 9.53e-3	0.12	0.90
	Soil brightness	1.48e-4 ± 1.77e-4	0.84	0.40
	BioClim PC1 (seasonality)	2.14e-5 ± 3.20e-6	6.67	<0.001***
	BioClim PC2 (aridity)	8.49e-5 ± 1.88e-5	4.50	<0.001***
	BioClim PC3 (temperature)	4.85e-5 ± 4.55e-5	1.06	0.29

782

783 Table 2: Non-linear regression analyses for investigating the relationship between the
784 reduction in cooling costs, temperature, and aridity. Slopes and standard errors are
785 presented and correspond to parameters in the exponential function $f(x) = a^{bx}$.
786

Temperature model	***a***	***b***
Slope ± SE	0.040 ± 0.005	0.097 ± 0.008
t-value	7.529	12.747
p-value	< 0.001	< 0.001
Aridity model		
Slope ± SE	0.1244 ± 0.0117	0.0017 ± 0.0003
t-value	10.636	4.926
p-value	< 0.001	< 0.001

787
788